12

Direct Numerical Simulation and Large Eddy Simulation of Compressible Turbulence

GORDON ERLEBACHER AND MOHAMMED Y. HUSSAINI

12.1 Abstract

An overview is given of recent work on the direct numerical simulation (DNS) and the large-eddy simulation (LES) of homogeneous compressible turbulent flows. Some DNS and LES results are presented. Some of the conclusions are shown to verify a recent theory which partially classifies the possible states of low Mach number turbulence. Finally, some issues regarding LES research in compressible turbulent flows are discussed.

12.2 Introduction

Compressible turbulence is currently the focus of attention in the fluid dynamics community, owing perhaps to, the renewed interest in the design of supersonic and hypersonic transport vehicles. In the quest to understand the basic physical mechanisms that distinguish compressible from incompressible turbulence, the body of knowledge in incompressible turbulence accumulated over the past several decades serves as a springboard to new levels of understanding. Today, researchers are studying compressible turbulent flows using direct numerical simulation (DNS) (Passot and Pouquet 1987; Blaisdell 1990; Lele 1990; Lee, Lele and Moin 1991; Sarkar, Erlebacher and Hussaini (1991a) ; Kida and Orszag 1990 a-b,1992) primarily. Some of these numerical results have been recently explained from a theoretical point of view (Tatsumi and Tokunaga 1974; Tokunaga and Tatsumi 1975; Erlebacher, Hussaini, Kreiss

and Sarkar 1990a; Sarkar, Erlebacher, Hussaini and Kreiss 1991b). Past theoretical work on compressible turbulent flows concentrated mostly on modifications of incompressible scaling laws to include Mach number effects (Zakharov and Sagdeev 1970; Kadomtsev and Petviashvili 1973; Moiseev, Sagdeev, Tur and Yanovskii 1977; L'vov and Mikhailov 1978a,b) Unfortunately, it is unlikely that the near future will bring about experiments detailed enough to confirm or reject any of these theories. However, with the explosion in supercomputer memory and speed, it is possible that DNS may soon provide some clues to spur theoretical research along the right direction.

In his seminal paper on supersonic turbulence, Kovasznay (1957) described the decomposition of compressible turbulence into acoustic, vortical and entropy modes. This interpretation of the eigenmodes of the flow remains a beacon in guiding the interpretation of results both in compressible turbulence and in compressible transition research. Another way to separate out the compressible and incompressible effects on the turbulence is to perform a Helmholtz decomposition on the velocity field (Moyal 1952; Passot and Pouquet 1987; Erlebacher et al. 1990a, Lee et al. 1991; Sarkar et al. 1991b). However, despite the progress made, much more work is required before the "incompressible" and "compressible" characteristics of the turbulent flows are fully classified. The cubic nonlinearities in the momentum equation and in the definition of kinetic energy add a degree of complexity to the interpretation of intermodal energy transfers. For example, we have become accustomed to a decomposition of the velocity field into Fourier components whose amplitude squared is correctly interpreted as the kinetic energy (or turbulent intensity) in the given mode. When the density fluctuations are taken into account in the definition of kinetic energy, it becomes necessary to make the distinction between the turbulent intensity, which involves only the velocity, and kinetic energy, which includes the effect of density fluctuations. Kida and Orszag (1990a,1992) have defined an energy spectrum based on the Fourier decomposition of $\mathbf{u}\sqrt{\rho}$. Although this reduces the kinetic energy to a quadratic form, the resulting interpretation of modal energy is not clearly related to physical mechanisms. However, any proposed decomposition will enhance our knowledge of the intricate physical mechanisms that are surely present in compressible turbulent flows.

Direct numerical simulations have uncovered several regimes of isotropic turbulence which are now under study. An original classification was attempted by Passot and Pouquet (1987), who found that strong

shocks are present when the fluctuating Mach number (M_t) is $O(1)$, while weak shocklets can be present even for small M_t. On the other hand, Feiereisen, Reynolds and Ferziger (1981) and Erlebacher, Hussaini, Speziale and Zang (1990b) performed DNS of compressible turbulence (with $M_t = 0.5$) which had *almost* incompressible statistical properties. The reason was brought out a few years later by Erlebacher et al. (1990a), who related the initial conditions of the flow to the characteristically different turbulent regimes. Since then, Kida and Orszag (1990a,b,1992) have considered both forced and unforced isotropic turbulence, and work has begun on homogeneous shear flow turbulence (Blaisdell 1990; Sarkar et al. 1991a).

The ultimate goal of current research on the physics of turbulence (besides academic interest) is to develop practical turbulence models applicable to complex flows of practical interest. Direct numerical simulations of such flows of aerodynamic interest are not practical even on today's fastest computers. The turbulence models are therefore a necessity in engineering applications. There are two standard approaches to turbulence modeling. In the first approach, the Navier–Stokes equations are averaged over time. As a consequence, the terms which are modeled contain both small and large spatial scales. This approach is known as Reynolds stress modeling. The application of Reynolds stress models to compressible flows has a long history and is not discussed in this chapter. Comprehensive reviews can be found in Cebeci and Smith (1974) and Speziale (1991). An alternative approach to turbulence modeling is to decompose the flow field into its large-scale (energy-containing) eddies and the presumably universal small scale eddies. While the dynamics of the large-scale eddies satisfy known evolution equations, there remain source terms, called subgrid-scale stress terms, which must be modeled. Subgrid-scale models are expected to be less sensitive to different large-scale flow conditions than their Reynolds stress counterparts if the assumption of small-scale universality proves to be valid. Of course, the price one pays for this increased generality is higher computational expense.

It is still too early to consider large eddy simulations (LES) of compressible flows as an engineering tool. However, once more reliable models are developed, LES databases can serve as an "exact" reference solution against which cheaper Reynolds stress models can be evaluated. This is pretty much the same relationship that exists between the existing DNS databases and the LES models under development.

In this chapter, we consider the advances in both the DNS and the

LES of compressible turbulence. These subjects are treated together since the numerical techniques that are used to perform the simulations are identical for both types of problem. In fact the subgrid-scale models are often incorporated into the DNS codes. To date, LES of compressible turbulence is based less on theory than on extensions of incompressible models to the compressible regime. As we demonstrate, these models, in the absence of shocks and/or shocklets, are quite capable of predicting reasonably well the decay rates of the turbulence and of the thermodynamics fluctuation rms levels. We conclude with some current issues that should be addressed in the near future. A discussion of recent LES advances can be found in Ferziger (1984). More recent reviews of the achievements of DNS and LES appear in Reynolds (1989) and Hussaini, Speziale and Zang (1989).

12.3 Direct numerical simulation

Direct numerical simulations seek the solution to the full compressible Navier–Stokes equations without any modeling. For reference, the Navier–Stokes equations (expressed in nondimensional form) are

$$\frac{\partial \rho}{\partial t} + \frac{\partial(\rho u_k)}{\partial x_k} = 0, \tag{1}$$

$$\frac{\partial(\rho u_k)}{\partial t} + \frac{\partial(\rho u_k u_l)}{\partial x_l} = -\frac{\partial p}{\partial x_k} + \frac{\partial \sigma_{kl}}{\partial x_l}, \tag{2}$$

$$\frac{\partial(\rho h)}{\partial t} + \frac{\partial(\rho h u_k)}{\partial x_k} = \frac{\partial p}{\partial t} + u_k \frac{\partial p}{\partial x_k} + \frac{\partial}{\partial x_k}\left(\kappa \frac{\partial T}{\partial x_k}\right) + \Phi, \tag{3}$$

respectively, where ρ is the mass density, $\mathbf{u}$ is the velocity vector, p is the thermodynamic pressure, μ is the dynamic viscosity, h is the enthalpy, T is the absolute temperature and κ is the thermal conductivity. The viscous stress σ_{kl} and the viscous dissipation Φ are defined by

$$\sigma_{kl} = -\frac{2}{3}\mu \frac{\partial u_j}{\partial x_j}\delta_{kl} + \mu\left(\frac{\partial u_k}{\partial x_l} + \frac{\partial u_l}{\partial x_k}\right), \tag{4}$$

$$\Phi = -\frac{2}{3}\mu\left(\frac{\partial u_j}{\partial x_j}\right)^2 + \mu\left(\frac{\partial u_k}{\partial x_l} + \frac{\partial u_l}{\partial x_k}\right)\frac{\partial u_k}{\partial x_l}, \tag{5}$$

respectively. Equations (1)–(3) must be supplemented with

$$p = \rho R T, \tag{6}$$

for an ideal gas , where R is the ideal gas constant. The dependence of the viscosity and thermal conductivity on the temperature must also be provided (i.e., relationships of the form $\mu = \mu(T)$ and $\kappa = \kappa(T)$ are

needed and these depend on the gas under consideration). Typically Sutherland's law is appropriate for the viscosity when the medium is air. The Prandtl number is assumed constant by most investigators.

The majority of compressible turbulence direct numerical simulations are concerned with homogeneous turbulence. In all cases, the boundary conditions are periodic in all coordinate directions. Homogeneous shear flow simulations are rendered periodic through the Rogallo transformation (Rogallo 1981). For a long time, only spectral methods were considered accurate enough for the numerical solution to the full Navier–Stokes equations. This was due to the low dissipation and dispersion errors of the method, which are very desirable characteristics of the numerical algorithm when one is performing direct numerical simulations. Indeed, one wishes to protect the structure of the smallest turbulent eddies from numerical dissipation and dispersion. Recently, however, high order finite-difference methods (Lele 1990; Shu, Erlebacher, Zang, Whitaker and Osher 1992) are gaining acceptance in the DNS community. Tests at Langley confirm the high accuracy of sixth order compact schemes applied to turbulence calculations (Shu et al. 1992). Besides its accuracy, the sixth order compact scheme is two times faster than the spectral algorithm when compared on identical numerical grids. However, except for the recent work of Lee et al. (1991) almost all investigators involved with the DNS of homogeneous turbulence still opt for Fourier collocation schemes (Canuto,Hussaini,Quarteroni and Zang 1988) because of their very desirable numerical properties (low truncation errors and exponential convergence).

Passot and Pouquet (1987) use the nonconservative form of the momentum equations and the conservative enthalpy equation. All terms are treated explicitly, except for the viscous terms, which are partially implicit. Time advancement is a combination of Crank–Nicolson and third order Adams–Bashforth. Erlebacher et al. (1990a,1992) consider initial conditions with very low turbulent Mach number. Consequently, they require an efficient implicit scheme with very low dispersion and dissipation errors to advance the acoustic terms in time. To this effect, a two-step time-split scheme is used. The first step integrates (with an explicit third order Runga–Kutta scheme) the full equations with a set of linear acoustic terms subtracted off. In the second step, the remaining set of (linear) equations is solved exactly in Fourier space. Thus, large time steps do not sacrifice accuracy, since the proper acoustic behaviour is accounted for in the implicit step. The only errors incurred are splitting errors and errors due to the (small) variation of the average

sound speed during the implicit stage. When time histories of statistical variables are required, the time step is decreased to resolve the sound waves.

Recently, Sarkar et al. (1991a) generated several direct numerical simulations of compressible homogeneous shear flow turbulence. Although a time-splitting algorithm similar to that of Erlebacher et al. (1990a) is possible, the simulations are currently fully explicit. The impact of the explicit scheme is not too high in the range of turbulent Mach numbers considered ($0.2 < M_t < 0.6$).

Feiereisen et al. (1981) performed the first DNS of compressible homogeneous turbulence. They described potential problems which could result from an improper discretization of the convective terms. They advocate rewriting the convective terms in the form

$$\frac{1}{2}\left[\frac{\partial(\rho u_k u_l)}{\partial x_l} + \rho u_l \frac{\partial u_k}{\partial x_l} + u_k \frac{\partial(\rho u_l)}{\partial x_l}\right]. \tag{7}$$

As noted by Feiereisen et al. (1981), if this form is employed, then a wide variety of numerical algorithms (including Fourier collocation), when applied to the inviscid compressible equations, conserve energy in addition to mass and momentum in the absence of time differencing (and splitting) errors. Fornberg (1975) discusses the conditions under which the nonsymmetric form of the convective equations maintains numerical stability. Recently, numerical simulations of supersonic boundary layer flows undergoing transition from a laminar to a turbulent state have demonstrated the unstable nature of both the conservation form $(\partial/\partial x_j)(\rho u_i u_j)$ and the nonconservative forms $\rho u_j(\partial u_i/\partial x_j)$ using a spectral collocation algorithm. Stability was achieved with Eq. (7). Note that the alternative form

$$\frac{1}{2}\left[\frac{\partial(\rho u_k u_l)}{\partial x_l} + \rho u_k \frac{\partial u_l}{\partial x_l} + u_l \frac{\partial(\rho u_k)}{\partial x_l}\right] \tag{8}$$

is also subject to instabilities. The reasons for this have not yet been ascertained. Zang (1990) discusses the relative merits of the different forms that can be taken by the convective operator in incompressible flows. He concludes that aliasing errors decrease substantially when the skew-symmetric form is used instead of either the rotational form $(\vec{\omega} \times \vec{u})$ or the nonconservative form $(\vec{u} \cdot \nabla \vec{u})$. However, he does not demonstrate an actual instability (using Eq. (7)) similar to one observed in recent simulations of transition of high speed flows. Blaisdell (1990) also discusses the aliasing properties of Eq. (7).

12.3.1 Initial Conditions

The choice of initial conditions in turbulent flow simulations is often more an art than a precise science. This is especially so for compressible turbulence simulations. Often, one can trace back a particular set of initial conditions to previous studies. In particular, incompressible turbulence initial conditions have been generalized to the compressible case without a full understanding of the consequences. For example, Feiereisen et al. (1981) and Erlebacher et al. (1992) choose a divergence-free initial velocity field and compute the initial pressure to ensure that the initial time derivative of the divergence of velocity will also be zero. Furthermore, the initial fluctuating density rms is set to zero. As explained by Erlebacher et al. (1990a) in the case of isotropic turbulence, these conditions lead to a very slow buildup of the compressibility effects on a convective $O(1)$ time scale. If one relaxes the condition that the initial time derivative of u_i be zero, and specifies random fluctuations for pressure, the flow reaches a quasi-equilibrium on an $O(M_t)$ time scale instead. Sarkar et al. (1991b) have shown that in homogeneous shear turbulence, significant compressibility develops as the turbulence Mach number increases, even though the initial velocity field is divergence-free and the initial pressure is chosen to ensure that the initial time derivative of the divergence of velocity is zero.

More general initial conditions were considered by Passot and Pouquet (1987) and adopted by Erlebacher et al. (1992). These allow the generation of weak and strong shocks, or simply acoustic waves of prescribed strength superimposed on an essentially nonlinear incompressible flow field. These initial conditions are based on a Helmholtz decomposition of the velocity field

$$\mathbf{u} = \mathbf{u}^I + \mathbf{u}^C, \tag{9}$$

where $\mathbf{u}^I$, $\mathbf{u}^C$ are respectively the solenoidal and irrotational components of velocity. At $t = 0$, the reference turbulent Mach number M_{t0}, the Reynolds number Re, the Prandtl number Pr, the rms levels of $\mathbf{u}_0^C$, $\mathbf{u}_0^I$, ρ_0, T_0 and the autocorrelation spectrum for ρ, T, $\mathbf{u}^C$ and $\mathbf{u}^I$ are imposed. The ratio of irrotational kinetic energy to total kinetic energy is also a free parameter and is denoted by χ. (The term "kinetic energy" actually refers to turbulent intensities.) A zero subscript refers to the initial state of the simulation. The energy spectrum of the density, temperature and velocity fluctuations are all given by

$$E(k) = k^4 e^{-2k^2/k_0^2}, \tag{10}$$

where k_0 corresponds to the spectrum peak. Strictly speaking the ini-

tially irrotational component of velocity should have an autocorrelation spectrum proportional to k^2 for low k to guarantee analyticity of the velocity field (Batchelor 1953). However, Erlebacher et al. (1992) did not feel that this would qualitatively influence the numerical results.

12.3.2 Results

In this section we present some numerical results obtained over the past few years. Some theoretical background is also provided.

Passot and Pouquet (1987) performed two- and three-dimensional DNS of compressible isotropic turbulence on 256^2 and 64^3 grids and were able to produce both weak and strong shocks. The presence or absence of the shocks was controlled solely by the initial conditions, whose influence can never completely vanish in decaying isotropic flow. They found three separate regimes. The weak Mach number regime ($M_t < 0.3$) has two subcomponents. If $\delta\rho/\rho \leq M_t^2$, the flow remains quasi-incompressible for all time. However, if $\delta\rho/\rho > M_t^2$, even by a small amount, the flow switches to a state which is mostly irrotational. Under these conditions weak shocks (negligible entropy jumps) can appear which propagate at the velocity of sound across the domain. The third regime is the strong-shock regime characterized by $M_t = O(1)$. Passot and Pouquet considered the decay laws of their spectra compared with those predicted by various statistical theories. Results were inconclusive, mainly because the simulations are still not capable of producing an inertial range. They also found that, in the strong-shock regime, there is a strong influence of the baroclinic torque in the vicinity of the shocks (for two-dimensional flows). In these cases, the $\nabla\rho$ and ∇p were found to be nearly perpendicular.

The ratio of irrotational kinetic energy to compressible potential energy is defined (Sarkar et al. 1991b) as

$$F = \frac{(\gamma M_t)^2 \ \chi}{p^{C2}} \tag{11}$$

where p^C is the compressible perturbation pressure defined by

$$p^C = p - p^I - < p >, \tag{12}$$

where $<>$ denotes a three-dimensional spatial average and where the pair ($\mathbf{u}^I$, p^I) satisfies the incompressible Navier–Stokes equations. It was shown in Sarkar et al. (1991b) that, for isotropic turbulence, F tends to unity after the initial acoustic transient dies, implying thereby the tendency toward equipartition between the kinetic and potential energy of the compressible component. This trend appears to hold for

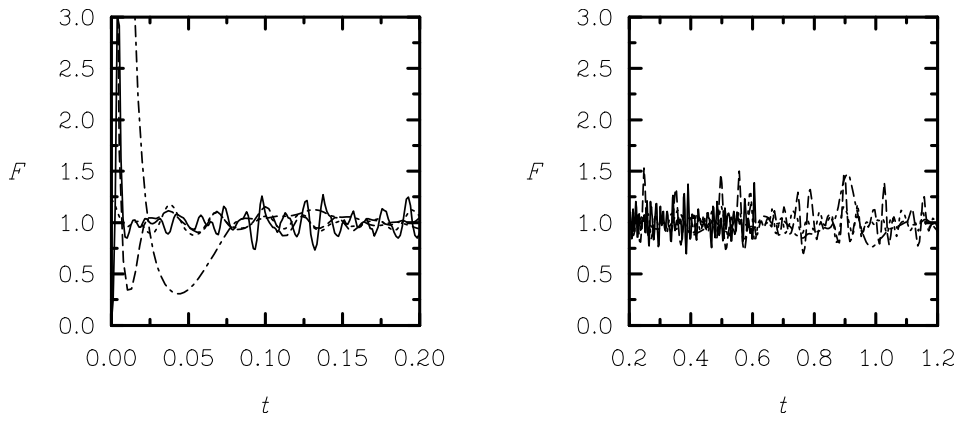

Fig. 1. Time history of F for four sets of initial conditions. (a) Acoustic time scale, (b) viscous time scale.

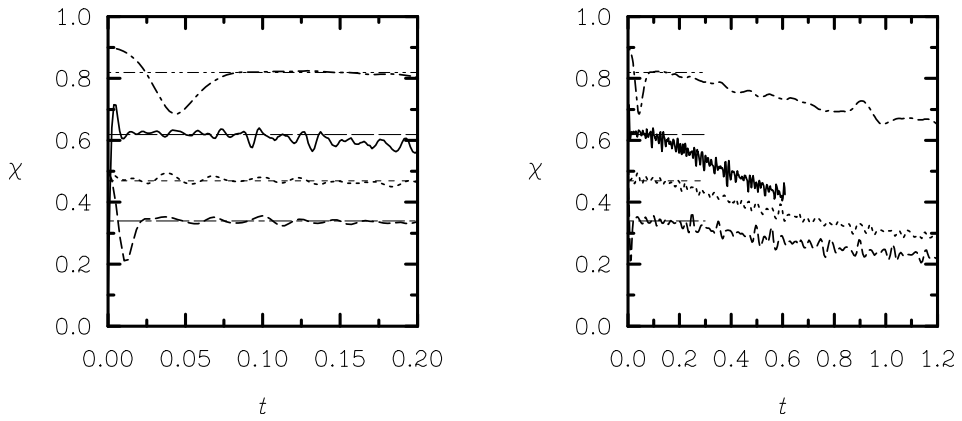

Fig. 2. Time history of the compressibility ratio χ for four sets of initial conditions. (a) Acoustic time scale, (b) viscous time scale.

homogeneous shear flow also (Sarkar et al. 1991a). Time histories of F and χ are presented in Figs. 1 and 2, starting from four widely different sets of initial conditions, all chosen to avoid

shocks on the acoustic time scale. The horizontal lines in Fig. 2 are the theoretical predictions for χ in the absence of viscous effects. Time histories on a longer (viscous) time scale are shown in Figs. 1b and 2b. Whereas F still oscillates around unity on the viscous time scale, χ can either increase or decrease. There is no available theory which can predict the long time scale evolution trends for χ.

Figures 3-4 show the time histories of the incompressible (E^I) and compressible (E^C) integrated turbulent intensities respectively from the same four simulations.

One notes the stronger oscillatory behavior in E^C, which is not sur-

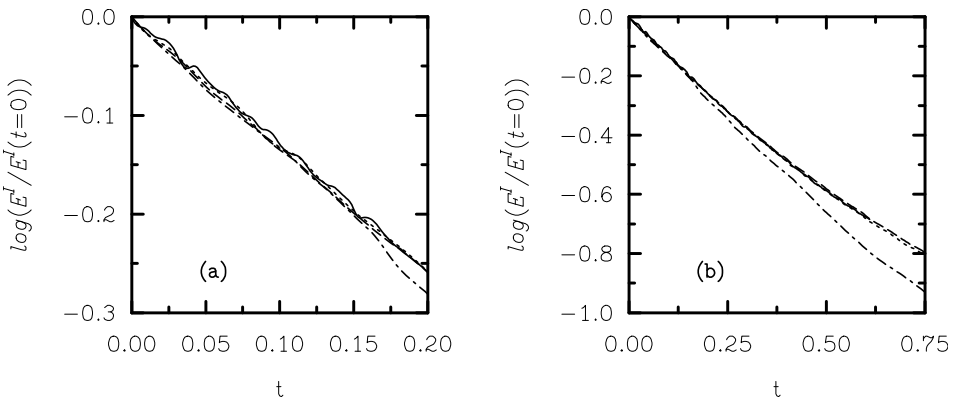

Fig. 3. Time history of solenoidal turbulent intensity. (a) Acoustic time scale, (b) viscous time scale.

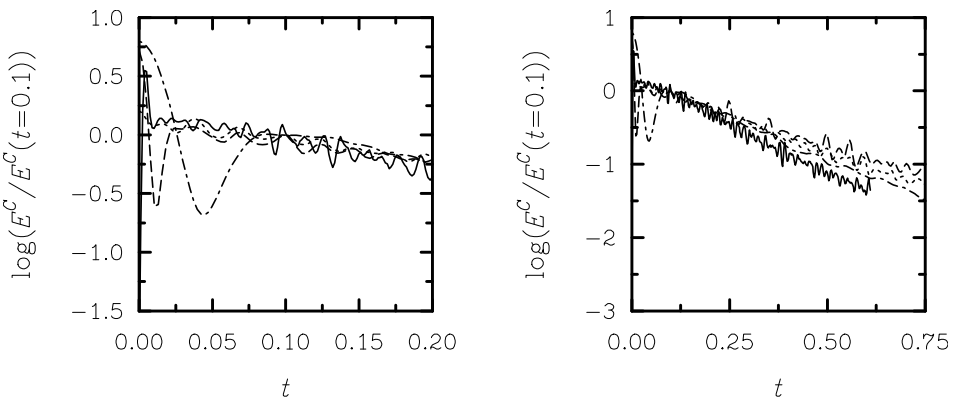

Fig. 4. Fig. 4. Time history of compressible bulent intensity. (a) Acoustic time scale, (b) viscous time scale.

prising given its wavelike behavior. Also of interest is the stronger dependence of E^C on initial conditions, even on a viscous time scale (compare Figs. 4a and 4b). Figure 5 compares the time histories of $\nabla \cdot \mathbf{u}$ without and with weak shocks in the flow. In the absence of shocks (or shocklets), the distribution of regions of expansion and compression is approximately equal (Fig. 5a). However, the presence of shocks leads to an asymmetry in the distribution of $\nabla \cdot \mathbf{u}$. Indeed, the preclusion of expansion shocks shows up as an asymmetry in Fig. 5b. The sharp negative peaks in the minimum divergence curve correspond to the crossing of two or more shocks. The width of the peaks is a function of both the shock speed and shock width. Lee et al. (1991) use the spatial average of velocity skewness to monitor the growth of shocks on the convective

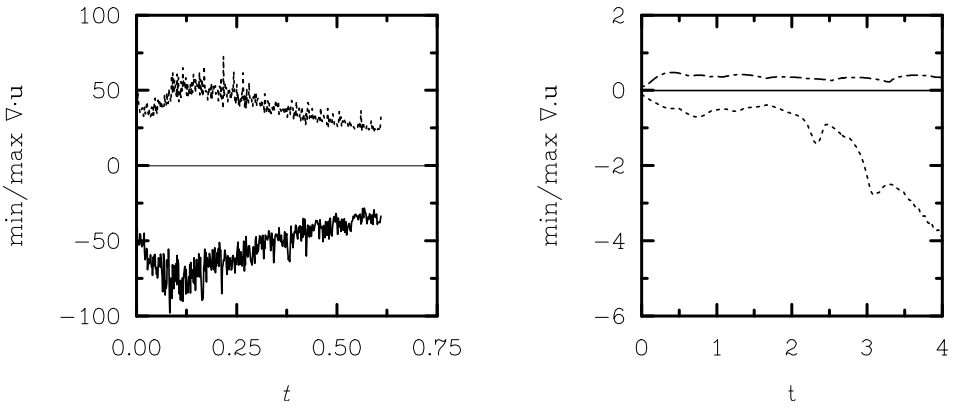

Fig. 5. Time history of $\nabla \cdot \mathbf{u}$ in a turbulent flow. (a) Without shocks, (b) with shocks.

time scale. These shocks tend to occur when the turbulent Mach number is $O(1)$.

Erlebacher et al. (1990a) are concerned primarily with the weak shock regime treated by Passot and Pouquet (1987). They seek to explain and quantify rigorously the relationship between initial conditions and the subsequent evolution of turbulence. By a careful asymptotic analysis, Erlebacher et al. (1990a) found that the presence of weak shocks is linked to initial flow conditions, which are out of acoustic equilibrium. For example, this situation arises for the initial conditions $M_t = 0.04$, $p_{rms} = 10\%$ and $\chi = 0.1$ where χ is the ratio of irrotational to solenoidal kinetic energy.

The compressible simulations of Kida and Orszag (1990b) highlight some interesting differences with Passot and Pouquet (1987). For example, Kida and Orszag find that in three-dimensional decaying turbulence, $\nabla\rho$ and ∇p are almost aligned in strong shock regions. These alignment properties in two-dimensional and three-dimensional turbulence are not currently explained. In the three-dimensional simulations, they found that the vorticity budget is dominated (overall) by the vortex stretching and the dissipation terms. However, in the shock regions, the compression and baroclinic terms produce vorticity, while the dissipation term depletes it.

Sarkar et al. (1991a) performed DNS of compressible, homogeneous shear flow turbulence. Initial conditions are imposed as in our isotropic turbulence simulations. Results indicate that compressibility reduces the growth of the turbulent kinetic energy. After performing a Helmholtz decomposition of the velocity and computing the associated pressure

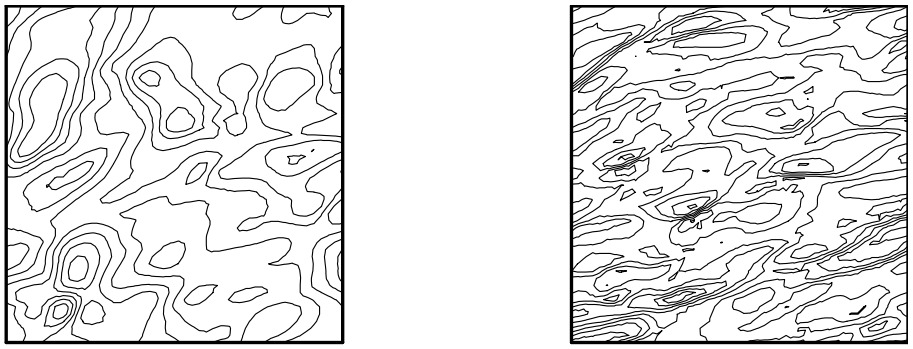

Fig. 6. (a) Incompressible component of pressure (p^I), and (b) compressible component of pressure (p^C) in compressible homogeneous shear flow turbulence. Shear rate $S = 15$.

fields, the authors found significant differences between the solenoidal and irrotational fields. The irrotational component acquires a wavelike character. This is most easily seen in the plots of p^I and p^C shown in Figs. 6a and 6b respectively. Preliminary flow visualizations of the magnitude of $\mathbf{u}^I$ and $\mathbf{u}^C$ have revealed the presence of streaks, although the character and orientation of the streaks are different for the two velocity fields. We are currently studying the properties of the streaks based on the invariants of the flow.

12.4 Large Eddy Simulation

Large eddy simulations incorporate subgrid-scale turbulence models into the Navier–Stokes equations in order to track accurately the small-scale phenomena that the numerical grid cannot resolve. One begins with a localized spatial average of the Navier–Stokes equations, which leads to unknown nonlinear terms that must be modeled. This approach is contrasted with Reynolds stress modeling, where one first averages the Navier–Stokes equations over time and then models the resulting unknown nonlinear terms. Under the (unproven) assumption that the character of turbulence in the small scales is somewhat universal, there is reason to believe that a good subgrid-scale model will be capable of treating a wider variety of complex geometrical configurations than their Reynolds-averaged counterparts. Large eddy simulations are still in their infancy and are still a long way from effectively proving to be reliable in realistic geometries. The greater computational expense of LES also makes it harder to run many simulations over a wide range

of parameters, which is essential to gain familiarity and intuition, two necessary ingredients for progress.

The large eddy simulations reported in this chapter are based on the following Favre-filtered continuity, momentum and energy equations (Speziale, Erlebacher, Zang and Hussaini 1992):

$$\frac{\partial \overline{\rho}}{\partial t} + \frac{\partial \overline{\rho}\tilde{u}_i}{\partial x_i} = 0,$$

$$\frac{\partial}{\partial t}(\overline{\rho}\tilde{u}_i) + \frac{\partial \overline{\rho}\tilde{u}_i\tilde{u}_j}{\partial x_i} = -\frac{\partial \overline{p}}{\partial x_i} + \frac{\partial \overline{\sigma}_{ij}}{\partial x_j} + \frac{\partial \tau_{ij}}{\partial x_j}, \tag{13}$$

$$\frac{\partial}{\partial t}(C_v\overline{\rho}\tilde{T}) + \frac{\partial C_v\overline{\rho}\tilde{u}_i\tilde{T}}{\partial x_i} = -\overline{p\,\frac{\partial u_i}{\partial x_i}} + \overline{\sigma_{ij}\frac{\partial u_i}{\partial x_j}} + \frac{\partial}{\partial x_i}\left(\overline{\kappa\frac{\partial T}{\partial x_i}}\right) - \frac{\partial Q_i}{\partial x_i},$$

where R is the ideal gas constant, C_v is the specific heat at constant volume, τ_{ij} is the subgrid-scale stress tensor and Q_i is the subgrid-scale heat flux. In Eqs. (13), an overbar represents a spatial filter whereas a tilde represents a mass-weighted or Favre filter, i.e.,

$$\tilde{\mathcal{F}} = \frac{\overline{\rho\mathcal{F}}}{\overline{\rho}}, \tag{14}$$

where $\mathcal{F}$ is any flow variable. These equations are obtained by applying a Gaussian filter to the full Navier–Stokes equations.

12.4.1 Subgrid-scale models

The subgrid scale stress tensor and subgrid scale heat flux are modeled as follows (Speziale et al. 1992; Erlebacher et al. 1990b):

$$\tau_{ij} = -C_C\overline{\rho}(\widetilde{\tilde{u}_i\tilde{u}_j} - \tilde{u}_i\tilde{u}_j) + 2C_R\overline{\rho}\Delta_f^2 II_{\tilde{S}}^{1/2}(\tilde{S}_{ij} - \frac{1}{3}\tilde{S}_{kk}\delta_{ij}) - \frac{2}{3}C_I\overline{\rho}\Delta_f^2 II_{\tilde{S}}\delta_{ij}, \tag{15}$$

$$Q_i = C_v\overline{\rho}\left(\widetilde{\tilde{u}_i\tilde{T}} - \tilde{u}_i\tilde{T} - \frac{C_R}{Pr_T}\Delta_f^2 II_{\tilde{S}}^{1/2}\frac{\partial\tilde{T}}{\partial x_i}\right), \tag{16}$$

where $II_{\tilde{S}} = \tilde{S}_{ij}\tilde{S}_{ij}$, Δ_f is the spatial filter width and C_R and C_I are model constants. In the incompressible limit, the subgrid-scale stress model (15) reduces to the linear combination model of Bardina, Ferziger and Reynolds (1983). The modified Navier–Stokes equations are solved with the numerical method discussed in Erlebacher et al. (1990a) modified to account for the eddy viscosity term. Time advancement of the modeled terms is fully explicit; therefore, the extra terms pose no difficulty.

The model constants C_C, C_I, C_R are related to the cross, Reynolds and

isotropic subgrid-scale stresses respectively. We also define a turbulent Prandtl number Pr_T in analogy with the standard Prandtl number.

Two subgrid-scale models that are gaining popularity include the dynamic model (Germano, Piomelli, Moin and Cabot 1990) and Lesieur's (1991) spectral viscosity model. Both models can be implemented in physical space. This requirement is necessary if LES concepts are to be useful in complicated geometrical configurations.

The objective of the dynamic model is to remove a major deficiency of the the Smagorinsky model wherein the model constants is a function of the particular flow under study. It is evident that if the model constant must be recalibrated for a different class of flows, the usefulness of the model is compromised. The dynamic model assumes a prescribed functional form for the unresolved scales (generally a Smagorinsky model), and furthermore assumes that this form is independent of the filter width. This is approximately true if the cutoff range is in the inertial range. (Without this latter hypothesis, LES simulations would generate grid-dependent results.) An algebraic identity derived by Germano (1990) relates the subgrid-scale stresses on two different coarse meshes. Substitution of the turbulence model into this identity provides the value of the "unknown" constant. It is shown by Germano (1990) that the model constant vanishes at solid boundaries, in laminar flow, and has the correct cubic dependence on the wall-normal coordinate near solid boundaries. In addition, the dynamic model allows backscatter (or inverse cascade) from the small to the larger scales in localized regions of the flow. The dynamic model has been extended to compressible homogeneous turbulence flows by Moin, Squires, Cabot, and Lee (1991). A summary of the compressible version of the model is given here. Its formulation closely follows the incompressible version found in Germano (1990).

Consider two filter operators $\overline{G}$ and $\hat{G}$. The former corresponds to the standard LES filter called the grid filter, while the latter is called the test filter. A composite filtering operator $\widehat{\overline{G}} = \overline{G}\widehat{G}$ is also defined. Concentrating our attention on the averaged Reynolds stress $u_i u_j$ in the momentum equations, we obtain, after filtering the momentum equations with $\overline{G}$ and $\widehat{\overline{G}}$, the unresolved stresses

$$\tau_{ij} = \overline{\rho}\,(\widetilde{u_i u_j} - \tilde{u}_i \tilde{u}_j) \tag{17}$$

and

$$T_{ij} = \widehat{\overline{\rho}}\,(\boxed{u_i u_j} - \boxed{u_i}\boxed{u_j}). \tag{18}$$

Here, we have defined the Favre average on the two grids by

$$\tilde{u_i} = \frac{\overline{\rho u_i}}{\overline{\rho}} \tag{19}$$

and

$$\boxed{u_i} = \frac{\widehat{\rho u_i}}{\hat{\rho}}. \tag{20}$$

Following Germano et al. (1990), it is easy to derive the identity

$$L_{ij} = T_{ij} - \tilde{\tau_{ij}}, \tag{21}$$

where L_{ij} has the interpretation of resolved turbulent stresses, i.e., those stresses whose scale lies between $\overline{\Delta}$ and $\widehat{\overline{\Delta}}$.

If one chooses a compressible Smagorinsky model to approximate the tensors T_{ij} and τ_{ij}, one can derive a Smagorinsky constant similar to that found in Germano et al. (1990). Various types of tensor contractions allow the separate modeling of the anisotropic and the isotropic components of the Reynolds stress without overly complicating the model. Whether the properties of the dynamic model (established for simple incompressible flows) hold for different types of compressible flows is one of many questions under investigation. Extensions of the dynamic model to handle the velocity–temperature correlations parallels the model for the subgrid Reynolds stresses.

The spectral viscosity model, developed by Lesieur (1991) has its origin in the eddy-damped quasi-normal Markovian (EDQNM) approximation to turbulence. Its original form is formulated in spectral space. A wave number k_C is defined beyond which the turbulence is considered unresolved. Scales smaller than k_C^{-1} are the subgrid scales. Subgrid-scale transfers of energy corresponding to wave triads with at least one wave number greater than the cutoff frequency k_C are computed with the help of EDQNM. This in turns leads to an approximate model for the subgrid-scale transfers which can be incorporated into the evolution equations written in spectral space. The success of Lesieur's model rests on the ability of EDQNM to predict the correct energy scaling laws for various turbulent variables. The extension of EDQNM (Marion 1988) to compressible flows leads to the possibility of extending Lesieur's model to compressibility effects.

We reemphasize that to be useful in practical configurations, subgrid-scale models should be formulated in physical space. Both the dynamic grid model and Lesieur's model can be so formulated.

12.4.2 Results

Before performing the LES, *a priori* estimates of the model constants are obtained by an analysis of the DNS data. To this end, the direct simulation data are first injected onto a coarser grid (16^3 or 32^3) and filtered. This reduced set of data corresponds to the results of an LES with an ideal subgrid-scale model. Under the assumption that our model is ideal, we effectively duplicate an LES without actually specifying the model. Using the coarse data, the various components of the subgrid-scale stresses are computed via Eq. (15). At the same time, the associated nonmodeled terms are computed on the fine DNS grid, followed by both coarsening and filtering. Model constants are then determined by comparing the coarsened exact stresses with the modeled stresses. This is accomplished in several ways, including least squares fits and comparisons of rms values of the different stress components. The analysis is performed on the tensor, vector and scalar levels. Full details are available in Erlebacher et al. (1992). Among the methods used to calculate the model constants, we find the most reliable to be the least squares fit of the full stress terms on the vector level. This means that the three components of $\tau_{ij,j}$ are compared individually. They are computed as a linear combination of the three individual subgrid-scale stresses with unknown coefficients. The least squares fit then allows the three constants to be determined. Of course, the cross-stress constant, C_C, must be unity for Galilean invariance of the model. Therefore, a procedure that determines all three constants was considered only valid if $C_C \approx 1$. The analysis produced results and correlations fully consistent with the results of Bardina et al. (1983). This is not surprising since the specified initial conditions led to turbulence, which remained quasi-incompressible for several large-eddy turnover times. A description of the initial conditions which lead to such situations is found in Erlebacher et al. (1990a).

Due to the low microscale Reynolds numbers of the DNS, there is no observable inertial range. As a consequence, the energy cascades directly from the large scales to the dissipation range. Since subgrid-scale models are expected to work best when the rate of energy flow is a constant, independent of the cutoff length scale, there is no reason to believe that the model constants will be independent of the LES grid resolution. This is borne out when comparing results of *a priori* analyses on 16^3 and 32^3 grids. The results are strongly grid dependent. However, we nonetheless felt sure that the sensitivity would not be as severe in a real LES. We chose the constants obtained with the 16^3 grid because the Smagorinsky constant C_R was closer to the value predicted by Bardina et al. (1983).

Unless specified otherwise, the constants used in the LES simulations are $C_C = 1$, $C_R = 0.012$, $C_I = 0.066$. The turbulent Prandtl number is taken to be 0.7.

The subgrid-scale model given by Eqs. (15) was tested by Erlebacher et al. (1990b) and by Zang, Dahlburg and Dahlburg (1991). Erlebacher et al. (1992b) compared the results of 96^3 DNS of isotropic decaying compressible turbulence with the results of LES on 32^3 grids. Both simulations had the following initial conditions: $Re = 250$, $\langle M_t^2 \rangle_0^{1/2} = 0.1$, $(\rho_{rms})_0 = 0$, $(T_{rms})_0 = 0.0626$ and a compressibility ratio $\chi_0 = 0.2$. Interestingly, this choice of parameters leads to an increase of χ. In general, however, χ is a decreasing function of time. The reason for the anomaly is not currently known and awaits further investigation.

The initial conditions for the LES were spectrally interpolated from the DNS results after the first peak in the time history of total enstrophy. Simulations were performed with a variety of subgrid-scale widths to confirm that a width $\Delta_f = 2$ gives the best results. We also varied the various model constants to study the sensitivity of the results with respect to the magnitude of the various modeled terms. We found that there is a fair degree of sensitivity. This confirms the need for subgrid-scale models more sophisticated than the models which implicitly result from the truncation errors of low order numerical schemes. One such model is the dynamic model mentioned earlier.

The biggest surprise was the insensitivity of the results to variations of 50% of C_I. We have therefore omitted this term from our model on the grounds that it has no effect. Zang et al. (1991), on the other hand, multiply C_I by 50, which results in a better match between the time histories of the rms density and the irrotational kinetic energy based on LES and DNS data. The initial conditions for this comparison were $\chi = 0.2$, $M_t = 0.1$. Unfortunately this improvement was not uniform when tried on simulation data based on runs with a range of initial conditions. Increasing C_I sometimes led to worse results than simply setting it to zero. Moin et al. (1991) have found at least one case where *a priori* testing suggests that C_I is indeed negligible, but DNS suggests otherwise. More investigation is clearly required. Therefore, it is still not clear whether this term should be part of the model. We do know, however, from the work of Sarkar et al. (1991b) that, within the framework of Reynolds stress modeling, the dilatational terms play an important role. It should therefore not come as a surprise if an extra term is required to model the isotropic components of the subgrid-scale

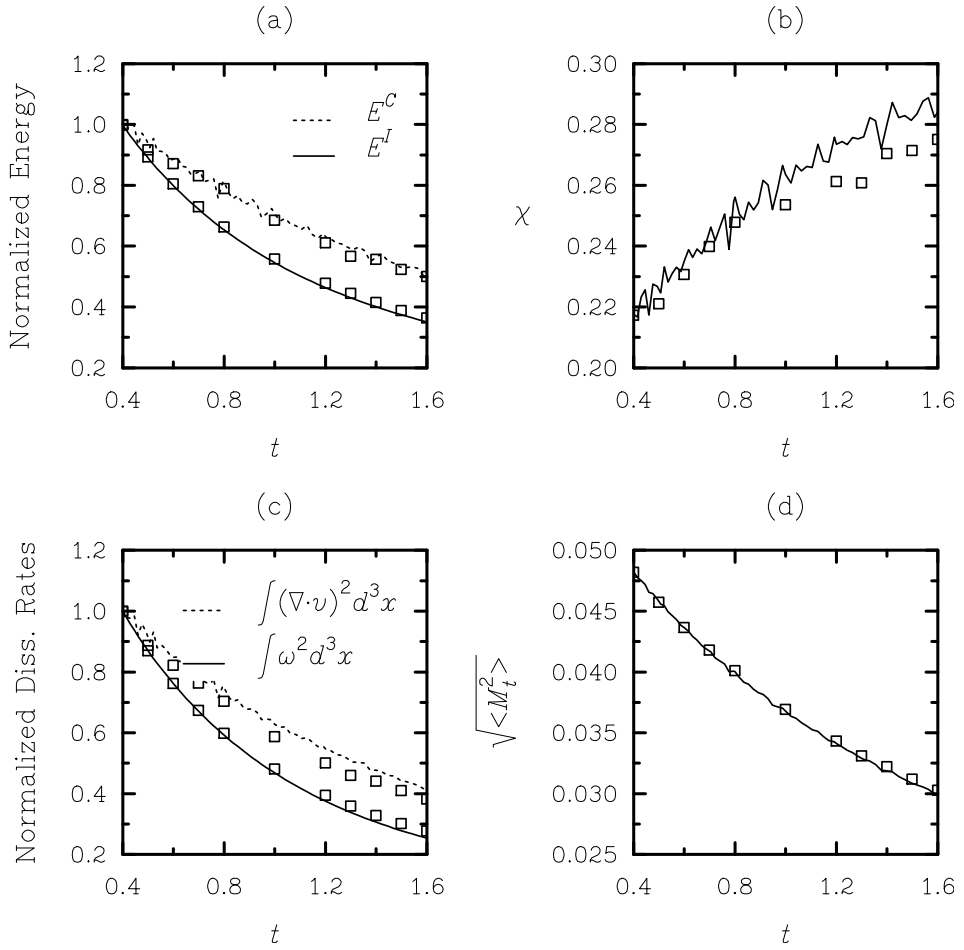

Fig. 7. Time histories of LES results on 32^3 grid with $\Delta_f = 2$. (a) solenoidal and irrotational kinetic energy, (b) χ, (c) $< (\nabla \cdot \mathbf{u})^2 >$ and $< \omega^2 >$, (d) M_t.

Reynolds stress. More work is clearly in order to establish leading order corrections to the current model.

Results show that the subgrid-scale model is capable of correctly predicting the decay rates of kinetic energy (both compressible and solenoidal) and of the thermodynamic variables (ρ, T, p). For illustration, Figure 7 shows time histories of several turbulent quantities obtained from the LES with a filter width $\Delta_f = 2$. In all the graphs, the symbols refer to the DNS results (coarsened and filtered) at selected times, while the solid lines refer to the results

of the LES. Figure 7a shows the good agreement of the decay rate of the incompressible and compressible total kinetic energy E^I and E^C. The agreement for E^I is not totally unexpected, since to leading or-

der, the evolution of the solenoidal velocity and that of the irrotational velocity are decoupled for small M_t. However, it is not clear why the agreement for E^C is so good since we are not specifically modeling compressibility, aside from mean density effects. If the general time evolution of terms directly related to compressibility is strongly linked to that of the incompressible turbulence, the developement of subgrid-scale models should be greatly facilitated. Large eddy simulations of compressible homogeneous shear flows should help us find out if this good fortune is linked to the isotropic nature of the flow or if it is more universal in character. A better measure of the model performance is given by the time history of χ (Fig. 7b). It is clear that the compressibility ratio is overpredicted. Therefore, the decay rate of E^C predicted by the LES is too low. In Fig. 7c, the decay rates of the variance of dilatation and vorticity are shown. Again, there is good agreement between DNS and LES. Good agreement of the decay rates of kinetic energy (large scales) and dissipation energies (small scales) is generally a good sign. Finally, time histories of the rms of density, temperature and pressure are shown in Fig. 7d. Considering the (almost) arbitrary choice of Pr_T, the agreement is quite good. Tests were conducted with different filter widths and different model constant values. For the particular LES under study, the C_R was optimal.

The effect of the model is most clearly demonstrated by performing a DNS on a 32^3 grid with the same initial conditions. This is equivalent to an LES with a filter width of $\Delta_f = 0$. Results are shown in Fig. 8 which exactly mirror the results presented in Fig. 7. The deterioration due to the lack of modeling is evident.

12.5 Conclusions

As emphasized in this brief overview, direct numerical simulations of several types of shock-free compressible turbulence have provided databases against which subgrid-scale models can be tested. Unfortunately, the Reynolds numbers that can be achieved in compressible flows are even lower than the already low Reynolds numbers inherent in today's best incompressible simulations. While we now know how to generate compressible turbulence with incompressible statistics, real flows may have significant compressibility effects (i.e., compressible mixing layers). Because of the low Reynolds numbers in the DNS, good subgrid-scale models at low Reynolds numbers may not automatically carry over to the larger ones.

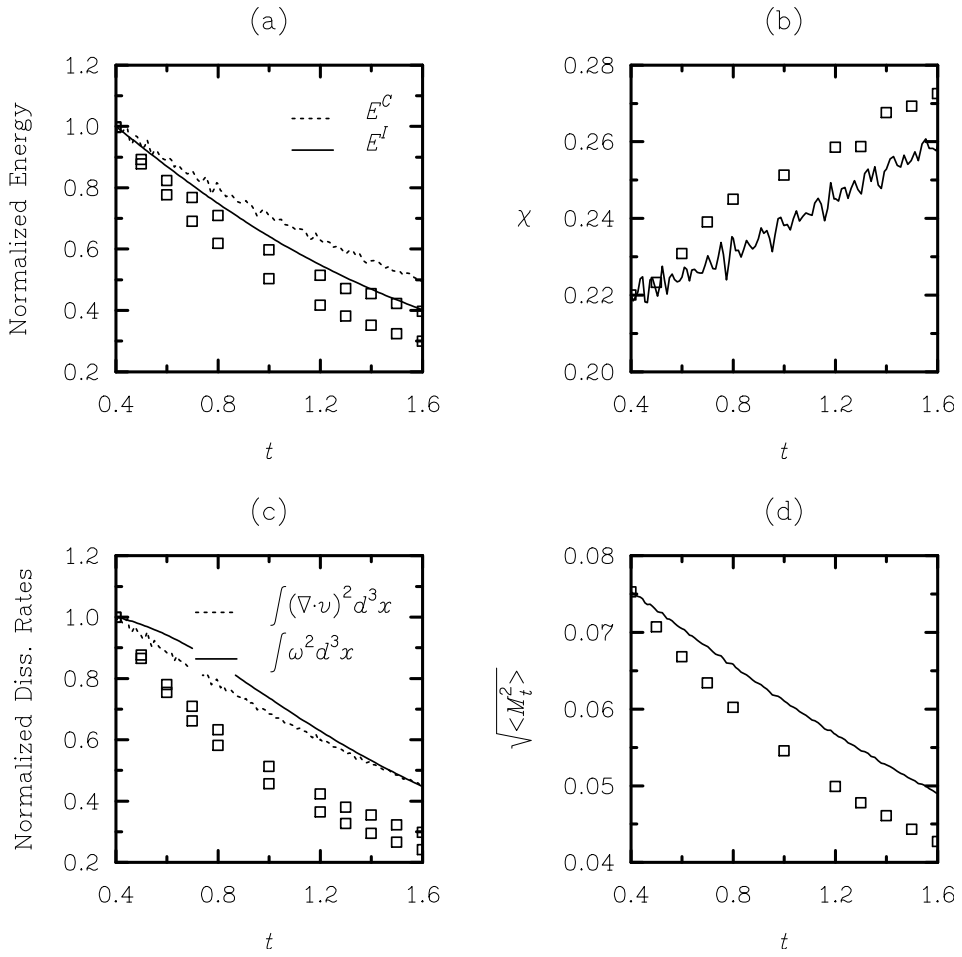

Fig. 8. Time histories of LES results on 32^3 grid with $\Delta_f = 0$. (a) solenoidal and irrotational kinetic energy, (b) χ, (c) $< (\nabla \cdot \mathbf{u})^2 >$ and $< \omega^2 >$, (d) M_t.

A couple of LES models have been developed recently to address this problem. They make use of information on the cascade process from large to small scales. In particular, the dynamic subgrid-scale model has no adjustable constants (they are computed from the resolved component of the flow). By its very construction, it holds great promise at the higher Reynolds numbers of practical engineering interest.

Research on LES is still in its infancy, and there are many obsticles to overcome. Within the next decade, the first large eddy simulations of flow over a three-dimensional wing are expected. A major issue will then become quantitative verification of the results.

References

Bardina, J., Ferziger, J.H., and Reynolds, W.C. (1983) Improved turbulence models based on large-eddy simulation of homogeneous, incompressible turbulent flows. Stanford University Technical Report TF-19.

Batchelor, G.K. (1953) *The Theory of Homogeneous Turbulence*. Cambridge University Press.

Blaisdell, G. (1990) Numerical simulation of compressible homogeneous turbulence. Ph.D Thesis, Stanford University.

Canuto, C., Hussaini, M.Y., Quarteroni, A. and Zang, T.A. (1988) *Spectral Methods in Fluid Dynamics*. Springer-Verlag.

Cebeci, T. and Smith, A.M.O. (1974) *Analysis of Turbulent Boundary Layers*. Academic Press.

Erlebacher, G, Hussaini, M.Y., Kreiss, H.O. and Sarkar, S. (1990a) The Analysis and Simulation of Compressible Turbulence. *Theor. Comput. Fluid. Dynam.* **2**, 73–95.

Erlebacher, G., Hussaini, M.Y., Speziale, C.G. and Zang, T.A. (1990b) On the large-eddy simulation of compressible turbulence. In proc. of the 12th Int. Conf. of Numerical Methods in Fluid Dynamics, Oxford University.

Erlebacher, G., Hussaini, M.Y., Speziale, C.G and Zang, T.A. (1992) Toward the large-eddy simulation of compressible turbulent flows. *J. Fluid Mech.* **238**, pp. 155-185.

Feiereisen, W.J., Reynolds, W.C. and Ferziger, J.H. (1981) Numerical simulation of compressible, homogeneous, turbulent shear flow. Report TF-13, Stanford University, Dept. of Mechanical Engineering.

Ferziger, J.H. (1984) Large eddy simulation: Its role in turbulence research. In *Theoretical Approaches to Turbulence*. Ed. D.L. Dwoyer, M.Y. Hussaini, and R.G. Voigt, Springer-Verlag.

Fornberg, B. (1975) On a Fourier methods for the integration of hyperbolic equations. *Siam J. Numer. Anal.* **12** (4), 509–528.

Germano, M. (1990) Averaging invariance of the turbulent equations and similar subgrid-scale modeling. CTR Manuscript 116, Stanford University.

Germano, M., Piomelli, U., Moin, P. and Cabot, W.H. (1990) A dynamic subgrid-scale eddy viscosity model. In *Studying Turbulence Using Numerical Simulation Databases – III.* CTR Manuscript 124, Stanford University.

Hussaini, M.Y., Speziale, C. and Zang, T.A. (1989) The potential and limitations of direct and large-eddy simulations, Comment 2. In *Wither Turbulence? Turbulence at the Crossroads*. Lecture Notes of Physics, vol. 357. Ed. J.L. Lumley, pp. 354-368.

Kadomtsev, B.B. and Petviashvili, V.I. (1973) Acoustic turbulence. *Sov. Phys. Dokl.* **18**, 115–116.

Kida, S. and Orszag, S. (1990a) Energy and spectral dynamics in forced compressible furbulence. *J. Sci. Computing* **5**, No. 2, 85-125.

Kida, S. and Orszag, S. (1990b) Enstrophy budget in decaying compressible turbulence. *J. Sci. Computing* **5**, No. 1, 1-34.

Kida, S. and Orszag, S. (1992) Energy and spectral dynamics in decaying compressible turbulence. *J. Sci. Computing* **7**, No. 1, 1-34.

Kovasznay, L.S.G. (1957) Turbulence in supersonic flows. *J. Aero. Sciences* **20**, (10), 657–682.

Lee, S., Lele, S.K. and Moin, P. (1991) Eddy shocklets in decaying compressible turbulence. *Phys. Fluids* **3**, (4), 657–664.

Lele, S.K. (1990) Compact finite-difference schemes with spectral-like resolution. CTR Manuscript 107, Stanford University.

Lesieur, M. (1991) *Turbulence in Fluids*. Kluwer.

L'vov, V.S. and Mikhailov, A.V. (1978a) Sound and hydrodynamic turbulence in a compressible liquid. *Sov. Phys. J. Exp. Theor. Phys.* **47**, 756–762.

L'vov, V.S. and Mikhailov, A.V. (1978b) Scattering and interaction of sound with sound in a turbulent medium. *Sov. Phys. J. Exp. Theor. Phys* **47**, 840–847.

Marion, J-D. (1988) Etude spectrale d'une turbulence isotrope compressible. Ph.D. thesis, Ecole Centrale de Lyon.

Moin, P., Squires, K., Cabot, W. and Lee, S. (1991) A dynamic subgrid-model for compressible turbulence and scalar transport. CTR Manuscript 124, Stanford University.

Moiseev, S.S., Sagdeev, R.Z., Tur, A.V. and Yanovskii, V.V. (1977) Structure of acoustic-vortical turbulence. *Sov. Phys. Dokl.* **22**, 582–584.

Moyal, J.E. (1952) The spectra of turbulence in a compressible fluid; Eddy turbulence and random noise. *Proc. Cambridge Phil. Soc.* **48**, part 1, 329–344.

Passot, A. and Pouquet, A. (1987) Numerical simulation of compressible homogeneous flows in the turbulent regime. *J. Fluid Mech.* **181** 441–466.

Reynolds, W.C. (1989) The potential and limitations of direct and large-eddy simulations. In *Wither Turbulence? Turbulence at the Crossroads*. Lecture Notes of Physics, vol. 357. Ed. J.L. Lumley, pp. 313–343.

Rogallo, S. (1981) Numerical experiments in homogeneous turbulence. NASA TM-81315.

Sarkar, S., Erlebacher, G. and Hussaini, M.Y. (1991a) Direct simulation of compressible turbulence in a shear flow. *Theor. Comput. Fluid Dynam.* **2**, 291–305.

Sarkar, S., Erlebacher, G., Hussaini, M.Y. and Kreiss, H.O. (1991b) The analysis and modeling of dilatational terms in compressible turbulence. *J. Fluid Mech.* **227**, 473–494.

Shu, C-W, Erlebacher, G., Zang, T.A., Whitaker, D. and Osher, S. (1992) High order ENO schemes applied to two- and three-dimensional compressible Euler and Navier–Stokes equations. *J. Appl. Num. Math.* **9**, 45–71.

Speziale, C.G. (1991) Analytical methods for the development of Reynold-stress closures in turbulence. *Ann. Rev. Fluid Mech.* **23**, 107–157.

Speziale, C.G., Erlebacher, G., Zang, T.A. and Hussaini, M.Y. (1988) The subgrid scale modeling of compressible turbulence. *Phys. Fluids* **31**, 940–942.

Tatsumi, T. and Tokunaga, H. (1974) One-dimensional shock-turbulence in a compressible fluid. *J. Fluid Mech.* **65**, 581.

Tokunaga, H. and Tatsumi, T. (1975) Interaction of plane nonlinear waves in a compressible fluid and two-dimensional shock-turbulence. *J. Phys. Soc. Japan* **38**, 1167–1179.

Yoshizawa, A. (1986) Statistical theory for compressible turbulent shear flows, with the application to subgrid modeling. *Phys. Fluids* **29**, 2152–2164.

Zakharov, V.E. and Sagdeev, R.Z. (1970) Spectrum of acoustic turbulence. *Sov. Phys. Dokl.* **15**, 439–441.

Zang, T.A. (1990) On the rotation and skew-symmetric forms for incompressible flow simulations. *Appl. Numer. Mathematics.* In press.

Zang, T.A, Dahlburg, R.B. and Dahlburg, J.P. (1991) Direct and large-eddy simulations of compressible, isotropic Navier–Stokes turbulence. NRL Memorandum Report 6799.